Interferometric characterization of the structured polarized light beam produced by the conical refraction phenomenon

Alba Peinado,[1] Alex Turpin,[1] Claudio Iemmi,[2] Andrés Márquez,[3,4] Todor K. Kalkandjiev,[1] Jordi Mompart,[1] and Juan Campos[1,*]

[1]*Departament de Física, Universitat Autònoma de Barcelona, 08193 Bellaterra, Spain*
[2]*Universidad de Buenos Aires, FCEyN - CONICET, Departamento de Física, 1428 Buenos Aires, Argentina*
[3]*Dept. de Física, Ing. de Sistemas y Teoría de la Señal, Univ. de Alicante, 03080 Alicante, Spain*
[4]*I.U. Física Aplicada a las Ciencias y las Tecnologías, Univ. de Alicante, 03080 Alicante, Spain*
[*]*juan.campos@uab.es*

Abstract: The interest on the conical refraction (CR) phenomenon in biaxial crystals has revived in the last years due to its prospective for generating structured polarized light beams, i.e. vector beams. While the intensity and the polarization structure of the CR beams are well known, an accurate experimental study of their phase structure has not been yet carried out. We investigate the phase structure of the CR rings by means of a Mach-Zehnder interferometer while applying the phase-shifting interferometric technique to measure the phase at the focal plane. In general the two beams interfering correspond to different states of polarization (SOP) which locally vary. To distinguish if there is an additional phase added to the geometrical one we have derived the appropriate theoretical expressions using the Jones matrix formalism. We demonstrate that the phase of the CR rings is equivalent to that one introduced by an azimuthally segmented polarizer with CR-like polarization distribution. Additionally, we obtain direct evidence that the Poggendorff dark ring is an annular singularity, with a π phase change between the inner and outer bright rings.

OCIS codes: (160.1190) Anisotropic optical materials; (260.1180) Crystal optics; (260.1440) Birefringence.

References and links

1. Q. Zhan, "Cylindrical vector beams: from mathematical concepts to applications," Adv. Opt. Photon. **1**(1), 1–57 (2009).
2. T. G. Brown and Q. Zhan, "Introduction: unconventional polarization states of light," Opt. Express **18**, 10775–10776 (2010).
3. J. P. Torres, "Quantum engineering of light," Opt. Pura Apl. **44**, 309–314 (2011).
4. K. Youngworth and T. Brown, "Focusing of high numerical aperture cylindrical-vector beams," Opt. Express **7**(2), 77–87 (2000).
5. R. Dorn, S. Quabis, and G. Leuchs, "Sharper focus for a radially polarized light beam," Phys. Rev. Lett. **91**(23), 233901 (2003).
6. C. J. R. Sheppard and A. Choudhury, "Annular pupils, radial polarization, and superresolution," Appl. Opt. **43**(22), 4322–4327 (2004).
7. Q. Zhan and J. Leger, "Focus shaping using cylindrical vector beams," Opt. Express **10**(7), 324–331 (2002).
8. S. Ramachandran, P. Kristensen, and M. F. Yan, "Generation and propagation of radially polarized beams in optical fibers," Opt. Lett. **34**(16), 2525–2527 (2009).
9. G. Gibson, J. Courtial, M. Padgett, M. Vasnetsov, V. Pas'ko, S. Barnett, and S. Franke-Arnold, "Free-space information transfer using light beams carrying orbital angular momentum," Opt. Express **12**(22), 5448–5456 (2004).
10. K. Ladavac and D. Grier, "Microoptomechanical pumps assembled and driven by holographic optical vortex arrays," Opt. Express **12**(6), 1144–1149 (2004).
11. F. Cardano, E. Karimi, S. Slussarenko, L. Marrucci, C. de Lisio, and E. Santamato, "Polarization pattern of vector vortex beams generated by q-plates with different topological charges," Appl. Opt. **51**(10), C1–C6 (2012).

#237787 Received 9 Apr 2015; revised 10 Jun 2015; accepted 11 Jun 2015; published 2 Jul 2015

12. C. E. R. Souza, J. A. O. Huguenin, and A. Z. Khoury, "Topological phase structure of vector vortex beams," J. Opt. Soc. Am. A **31**(5), 1007–1012 (2014).
13. X. Zheng, A. Lizana, A. Peinado, C. Ramírez, J. L. Martínez, A. Márquez, I. Moreno, and J. Campos, "Compact LCOS-SLM based polarization pattern beam generator," J. Lightwave Technol. in press.
14. H. I. Sztul and R. R. Alfano, "Double-slit interference with Laguerre-Gaussian beams," Opt. Lett. **31**(7), 999–1001 (2006).
15. V. G. Denisenko, A. Minovich, A. S. Desyatnikov, W. Krolikowski, M. S. Soskin, and Y. S. Kivshar, "Mapping phases of singular scalar light fields," Opt. Lett. **33**(1), 89–91 (2008).
16. A. Dudley, G. Milione, R. R. Alfano, and A. Forbes, "All-digital wavefront sensing for structured light beams," Opt. Express **22**(11), 14031–14040 (2014).
17. M. V. Berry and M. R. Jeffrey, "Conical diffraction: Hamiltons diabolical point at the heart of crystal optics," Prog. Opt. **50**, 13–50 (2007).
18. A. Turpin, Y. V. Loiko, T. K. Kalkandjiev, H. Tomizawa, and J. Mompart, "Wave-vector and polarization dependence of conical refraction," Opt. Express **21**(4), 4503–4511 (2013).
19. T. Kalkandjiev and M. Bursukova, "Conical refraction: an experimental introduction," Proc. SPIE **6994**, 69940B (2008).
20. A. Turpin, Y. Loiko, T. K. Kalkandjiev, and J. Mompart, "Free-space optical polarization demultiplexing and multiplexing by means of conical refraction," Opt. Lett. **37**(20), 4197–4199 (2012).
21. A. Peinado, A. Turpin, A. Lizana, E. Fernández, J. Mompart, and J. Campos, "Conical refraction as a tool for polarization metrology," Opt. Lett. **38**(20), 4100–4103 (2013).
22. D. P. O'Dwyer, C. F. Phelan, K. E. Ballantine, Y. P. Rakovich, J. G. Lunney, and J. F. Donegan, "Conical diffraction of linearly polarised light controls the angular position of a microscopic object," Opt. Express **18**(26), 27319–27326 (2010).
23. A. Turpin, V. Shvedov, C. Hnatovsky, Y. V. Loiko, J. Mompart, and W. Krolikowski, "Optical vault: a reconfigurable bottle beam based on conical refraction of light," Opt. Express **21**(22), 26335–26340 (2013).
24. M. Born and E. Wolf, *Principles of Optics* (Cambridge Univ. Press, UK, 1997).
25. A. M. Belskii and A. P. Khapalyuk, "Internal conical refraction of bounded light beams in biaxial crystals," Opt. Spectrosc. **44**, 436–439 (1978).
26. A. M. Belskii and A. P. Khapalyuk, "Propagation of confined light beams along the beam axes (axes of single ray velocity) of biaxial crystals," Opt. Spectrosc. **44**, 312–315 (1978).
27. A. M. Belskii and M. A. Stepanov, "Internal conical refraction of light beams in biaxial gyrotropic crystals," Opt. Commun. **204**(1-6), 1–6 (2002).
28. P. Kurzynowski, W. A. Woźniak, and M. Szarycz, "Geometric phase: two triangles on the Poincaré sphere," J. Opt. Soc. Am. A **28**(3), 475–482 (2011).
29. J. L. Martínez-Fuentes, J. Albero, and I. Moreno, "Analysis of optical polarization modulation systems through the Pancharatnam connection," Opt. Commun. **285**(4), 393–401 (2012).
30. T. Wakayama, O. G. Rodríguez-Herrera, J. S. Tyo, Y. Otani, M. Yonemura, and T. Yoshizawa, "Generation of achromatic, uniform-phase, radially polarized beams," Opt. Express **22**(3), 3306–3315 (2014).
31. J. C. Loredo, O. Ortíz, R. Weingärtner, and F. De Zela, "Measurement of Pancharatnam's phase by robust interferometric and polarimetric methods," Phys. Rev. **80**(1), 012113 (2009).
32. D. Malacara, M. Servín, and Z. Malacara, *Interferogram analysis for optical testing* (CRC Press, 2005), Chap. 7.
33. D. H. Goldstein, *Polarized Light* (CRC Press, 2010).
34. M. V. Berry, "Conical diffraction asymptotics: Fine structure of Poggendorff rings and axial spike," J. Opt. A, Pure Appl. Opt. **6**(4), 289–300 (2004).
35. A. Turpin, J. Polo, Y. V. Loiko, J. Küber, F. Schmaltz, T. K. Kalkandjiev, V. Ahufinger, G. Birkl, and J. Mompart, "Blue-detuned optical ring trap for Bose-Einstein condensates based on conical refraction," Opt. Express **23**(2), 1638–1650 (2015).
36. A. Turpin, Y. V. Loiko, T. K. Kalkandkiev, H. Tomizawa, and J. Mompart, "Super-Gaussian conical refraction beam," Opt. Lett. **39**(15), 4349–4352 (2014).
37. Y. V. Loiko, A. Turpin, T. K. Kalkandjiev, E. U. Rafailov, and J. Mompart, "Generating a three-dimensional dark focus from a single conically refracted light beam," Opt. Lett. **38**(22), 4648–4651 (2013).
38. A. Turpin, Y. V. Loiko, A. Peinado, A. Lizana, T. K. Kalkandjiev, J. Campos, and J. Mompart, "Polarization tailored novel vector beams based on conical refraction," Opt. Express **23**(5), 5704–5715 (2015).

1. Introduction

In recent times research dealing with beams with spatially inhomogeneous polarization and/or phase distributions has attracted much attention, both from a fundamental point of view and also because of the novel capabilities offered with a potential to be used in a number of modern photonics applications ranging from sensing, nanoscale imaging, quantum nano-optics, to metrology and nanolithography [1–3]. Cylindrical vector (CV) beams, with radial or azimuthal polarizations, and/or with vortex-like spatial phase distributions have received the greatest attention. CV beams have already found application in sharper focusing [4,5], in

#237787 Received 9 Apr 2015; revised 10 Jun 2015; accepted 11 Jun 2015; published 2 Jul 2015

optical imaging [6] or in focal field engineering [7], as well as in the generation of eigenmodes in cylindrical resonators and optical fibers [8]. Vortex beams have been also used in optical communications [9] or in particle trapping and manipulation [10]. In fact, CV and vortex beams are very much related and beams combining both structures in polarization and in phase, so-called vector vortex beams have been also produced [11,12]. There can be found different techniques to generate these new types of light beams, as reviewed by Zhan et al. [1]. Also, novel systems and strategies able to produce spatial light distributions with a high number of degrees of freedom have been proposed, as the one reported recently by Zheng et al. [13]. Together with the capability of generating these beams, measurement techniques are also required to validate the actual spatial complex amplitude and polarization structure, namely interferometric [14,15] or polarimetric [16].

Other types of beams with unconventional spatial inhomogeneous distributions are also receiving strong consideration as presented by Brown and Zhan [2]. This is the case of the unusual beams produced by conical refraction (CR) in a biaxial crystal (BC) [17–19], already applied in free-space optical communications [20], in polarization metrology [21] or in particle trapping [22,23]. CR is a fundamental phenomenon in optics with two basic manifestations, internal and external CR, as presented in the classical textbook by Born and Wolf [24]. In the former, a narrow beam of light, which enters a BC along one of the optic axes, evolves as a hollow slanted cone and on the exit facet refracts as a hollow cylinder. If the incident beam is unpolarized or circularly polarized, then it becomes decomposed in linearly polarized states along the ring of the cylinder, each point on the ring being associated with a specific linear state of polarization where diametrically symmetric points possess orthogonal linear polarization.

Complete calculation of CR according to Fourier analysis has been performed by Belsky and coauthors [25–27] and by Berry and coauthors [17] together with experimental demonstrations [19]. Most of the studies in the literature have dealt with the inhomogeneous polarization and intensity structure in CR beams, but no attention has been focused onto the phase distribution. To meet this goal a direct approach is to build an interferometer where the CR beam interferes with a reference beam. Since the CR beam is not scalar, i.e. it shows inhomogenous polarization structure, special care is necessary to avoid misinterpretation of the results due to additional Pancharatnam-Berry geometric phases [28–30] arising from the different polarizations in the reference and sample beams. On its turn, measurement of the geometric phase can be accomplished by using interferometers or polarimeters [31].

In this article we build a Mach-Zehnder interferometer to measure the phase distribution across the ring structure created by CR at the focal plane. We apply the well-known phase-shifting technique [32] to reconstruct the spatial map of phase distribution across the wavefront and not just the interferogram as it is typically the case in most of the works. In Section 2 we introduce the diffractive theory of CR and, in order to take into account any geometric phase introduced by the interference with the reference beam we also derive the corresponding analytical expressions using the Jones formalism for polarization [33]. In Section 3, the corresponding experimental results are obtained using a composed linear polarizer whose structure resembles the polarization structure of the CR beam. In Section 4, we proceed with the interferometric experiment with the CR beam and results are analyzed. Finally, conclusions are drawn in Section 5.

2. Theoretical background

2.1 Diffractive solution of conical refraction

The theory of CR for focused beams was developed by Belsky and Khapalyuk [25] and reformulated in an elegant way by Berry [34]. For a homogeneously polarized and cylindrically symmetric input beam, light's intensity distribution behind the BC is given by

#237787 Received 9 Apr 2015; revised 10 Jun 2015; accepted 11 Jun 2015; published 2 Jul 2015

$$I(\rho, Z) = |B_0|^2 + |B_1|^2, \tag{1}$$

where

$$B_0(\rho, Z) = \frac{1}{2\pi}\int_0^\infty \eta a(\eta) e^{-i\frac{Z\eta^2}{2n}} J_0(\eta\rho)\cos(\eta\rho_0)d\eta, \tag{2}$$

$$B_1(\rho, Z) = \frac{1}{2\pi}\int_0^\infty \eta a(\eta) e^{-i\frac{Z\eta^2}{2n}} J_1(\eta\rho)\sin(\eta\rho_0)d\eta, \tag{3}$$

$$a(\eta) = \int_0^\infty \rho E(\rho) J_0(\eta\rho)d\rho, \tag{4}$$

being $\rho = r/w_0$ and $Z = z/z_R$ the radial and longitudinal components in cylindrical coordinates normalized to the beam waist w_0 and the Rayleigh length z_R of the input beam. $a(\eta)$ is the radial part of the 2D transverse Fourier transform of the input beam $\vec{E}(\rho) = E(\rho)\vec{e}_0$, where $\eta = |k_T| w_0$ is the modulus of the transverse wave-vector components projected onto the entrance surface of the crystal, and J_q denotes the Bessel function of order *q*. In our work we restrict to beams with Gaussian transverse profile for which $a(\eta) = \exp(-\eta^2/4)$ [35]. Note that Eqs. (2,3) the factor $\rho_0 = R_0/w_0$ rules the evolution of the CR beam emerging from the BC, where R_0 is the geometrical approximation of the CR ring radius that depends on the principal refractive indices of the material [17,19]. For $\rho_0 = 0$, i.e. for null birefringence, the output beam keeps the shape of the Gaussian input beam. As ρ_0 increases, the birefringence provided by the BC becomes appreciable and the transverse intensity pattern at the focal plane forms a Super-Gaussian beam ($\rho_0 = 0.45$ [36]), a doughnut like beam ($\rho_0 = 0.92$ [37]) and other related patterns [38]. For $\rho_0 >> 1$, which covers most of the studies related to CR, the transverse intensity pattern at the focal plane forms a pair of concentric bright rings split by a null intensity ring, known as the Poggendorff dark ring [34]. The state of polarization of the rings is linear at every point with the azimuth rotating by π rad for a complete turn along the rings [19, 38]. In this work we restrict to this condition of $\rho_0 >> 1$ for which the Poggendorff dark ring is formed and demonstrate experimentally that it is an annular singularity separating the inner and outer rings of CR.

2.1 Theoretical analysis of the interferometric experiment

In order to analyze the structure of the phase associated with the wavefront originated by CR in the BC we will perform interferometric experiments where the CR beam is the sample beam, which interferes with a reference beam. In general the two beams have a different state of polarization (SOP). In the following we analyze some specific situations of interference of two beams with different SOPs. The theoretical results obtained will help us to interpret the experiments in Sections 3 and 4. First thing to consider is that the phase-difference δ between two beams with a different polarization participating in interference is given by [28]:

$$\delta = \arg(\vec{J}_1^* \cdot \vec{J}_2), \tag{5}$$

where $\vec{J}_1$ and $\vec{J}_2$ denote the complex Jones vectors of two electric fields describing the interfering light waves, and the argument of their hermitic scalar product is the phase difference. In the case of two interfering beams with equal SOPs, a non-zero phase difference originates from their relative time delay. However, if the two beams have different SOPs, a non-zero phase difference is still possible even if there is no time delay. In this case, the

#237787 Received 9 Apr 2015; revised 10 Jun 2015; accepted 11 Jun 2015; published 2 Jul 2015

phase-difference is strictly given by the projection between the two SOPs and thus has a pure geometric origin. This is the so-called geometric phase, which is related to the Pancharatnam-Berry phase [28], and provides a means to establish when two beams with a different SOP can be considered to be in phase. This distinction between the geometric and non-geometric origin of the phase-difference is of relevance for the purpose of the paper.

Let us consider an amplitude division interferometer, such as the Mach-Zehnder, and the two following experiments sketched in Figs. 1(a) and (b). In both experiments a plane wave with a right-handed circular SOP is incident onto a beam-splitter, which produces a reflected and a transmitted beam along the two arms of the interferometer. We consider the beam-splitter to be non-polarizing, and the transmitted and reflected beams to be respectively the sample and reference beams. The reflected (reference) beam is unchanged in the first experiment, Fig. 1(a), while in the second experiment, it traverses a linear polarizer whose transmission axis is at an angle β_1 (expressed with respect to the vertical of the lab-reference system). In the two experiments the transmitted (sample) beam traverses a linear polarizer whose transmission axis is at an angle β_2. Both the sample and reference beam will be finally brought together to interfere with a non-polarizing beam-splitter.

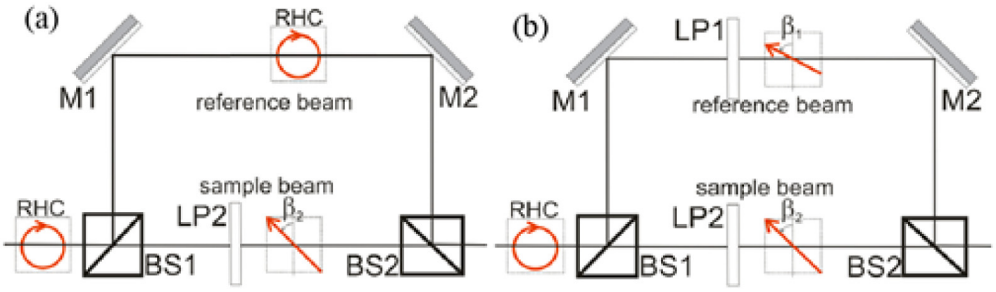

Fig. 1. Diagrams for the first (a) and second (b) experiment in the Mach-Zehnder interferometer analyzed in the text. Thin arrows (in red) represent the polarization state. BSi: Non polarizing beam splitters. LPi: Linear polarizers oriented at β_i with respect to the vertical.

The experiments expressed in Fig. 1 can be analytically described by means of the Jones formalism for polarization [33]. In this formalism the right-handed circularly (RHC) SOP is given by $\vec{J}_{RHC} = (1, i)^T$, which corresponds to the polarization of the input beam $\vec{J}_{in}$ in the interferometer. When this beam transmits through a linear polarizer with its transmission axis at an angle β with respect to the X-axis in the system (along the vertical of the lab-reference system) we obtain an output beam linearly polarized whose expression can be calculated from the following product,

$$\vec{J}_{out} = R(-\beta) P_X R(\beta) \vec{J}_{in}, \tag{6}$$

where $R(\beta)$ and P_X are respectively the rotation and the X-polarizer matrices,

$$R(\beta) = \begin{pmatrix} \cos\beta & \sin\beta \\ -\sin\beta & \cos\beta \end{pmatrix}, \tag{7}$$

$$P_X = \begin{pmatrix} 1 & 0 \\ 0 & 0 \end{pmatrix}. \tag{8}$$

And the Jones output vector $\vec{J}_{out}$ is given by,

#237787 Received 9 Apr 2015; revised 10 Jun 2015; accepted 11 Jun 2015; published 2 Jul 2015

$$\vec{J}_{out} = \exp(i\beta)\begin{pmatrix}\cos\beta\\ \sin\beta\end{pmatrix} = \vec{J}_{LP}(\beta), \tag{9}$$

labeled as $\vec{J}_{LP}(\beta)$ expressing that the SOP is linearly polarized at an angle β. Note that no time delay has been added in the expressions for $\vec{J}_{RHC}$ and $\vec{J}_{LP}(\beta)$, thus the phase difference obtained through Eq. (5) when applying any of these SOP expressions is purely of a geometric origin. We have now all the ingredients to calculate the interference in both experiments presented in Fig. 1.

In the first experiment the scalar product of the two interfering beams is,

$$\vec{J}^{*}_{RHC} \cdot \vec{J}_{LP}(\beta_2) = 1, \tag{10}$$

and both beams are in phase, i.e

$$\delta = \arg\left(\vec{J}^{*}_{RHC} \cdot \vec{J}_{LP}(\beta_2)\right) = 0. \tag{11}$$

In the second experiment, the projection between the two interfering electric fields is given by,

$$\vec{J}^{*}_{LP}(\beta_1) \cdot \vec{J}_{LP}(\beta_2) = e^{i(\beta_2-\beta_1)}\cos(\beta_2-\beta_1), \tag{12}$$

and the phase-difference δ results as,

$$\delta = \begin{Bmatrix}\beta_2-\beta_1; \cos(\beta_2-\beta_1)\geq 0\\ \beta_2-\beta_1+\pi; \cos(\beta_2-\beta)<0\end{Bmatrix}. \tag{13}$$

Then depending on the relative orientation of the polarizers we obtain a π radians phase jump in the interference phase δ, which is purely of geometric origin. This is an interesting result which will be used in the experiments in the following Sections. To simplify the analysis let us consider the orientation between the two linearly polarized SOPs in the interfering beams almost orthogonal, with $\beta_1 = 0°$ and with the second beam at $\beta_{2,\pm} = \pi/2 \pm \alpha$, i.e. slightly deviated an angle α from the orthogonal condition. Taking into account the $\pm$ sign the projection between the two interfering electric fields can be expressed as,

$$\vec{J}^{*}_{LP}(\beta_1 = 0) \cdot \vec{J}_{LP}(\beta_{2,\pm}) = \exp\left(i\pi \mp i\left(\pi/2+\alpha\right)\right)\sin\alpha, \tag{14}$$

And the phase-difference δ is given in either case by,

$$\delta_{\pm} = \pi \mp \left(\frac{\pi}{2}+\alpha\right). \tag{15}$$

The difference between the plus and minus signs is then,

$$\Delta\delta = \delta_{-} - \delta_{+} = \pi + 2\alpha, \tag{16}$$

i.e. we obtain a π radians phase jump when α is close to zero. The results obtained in Eqs. (11), (13) and (16) will be our basic tools to interpret any non-geometric origin in the phases measured in Sections 3 and 4.

#237787 Received 9 Apr 2015; revised 10 Jun 2015; accepted 11 Jun 2015; published 2 Jul 2015

3. Experimental results with a variable transmission axis polarizer

For the experiments in Sections 3 and 4 we consider a Mach-Zehnder interferometer illuminated with a He-Ne laser (wavelength 633 nm), where one of the mirrors along the reference beam is mounted onto a piezoelectric actuator, used as a phase-shifter. Both the sample and reference beams are recombined by a non-polarizing beam-splitter at the exit of the interferometer, and a CCD camera afterwards captures the interferogram between the two beams. The phase difference at each point across the spatial aperture of the interfering beams is then extracted by applying phase-shifting techniques, i.e. four interferograms are acquired with different phase shifts of the reference (0, π/2, π, 3π/2), and by combining them the phase distribution is obtained.

The sample beam in Section 4 is the one produced by CR in a BC. In the present Section the sample beam is produced by a sector-composed polarizer whose structure emulates that of the linear SOPs produced by the CR phenomenon along the ring at the focal plane, qualitatively described in the Introduction. This serves to have a proper calibration of the experimental setup so that the results eventually obtained with the crystal in Section 4 can be properly interpreted.

In Fig. 2 we show a diagram for the spatially varying polarizer, which in the rest of the paper we will call "conical refraction polarizer" (CRP). It is divided in eight sectors with a relative difference of 22.5° in the orientation of the transmission axis between consecutive sectors and where symmetric sectors possess orthogonal orientations. The transmission axis in each sector in the diagram corresponds to the green arrow line, whose orientation is indicated by green number nearby.

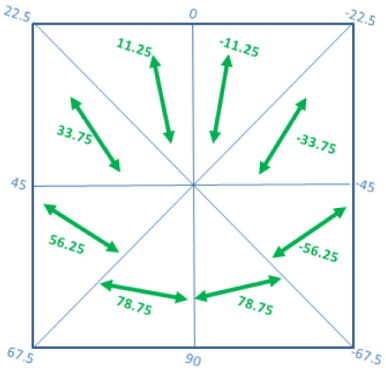

Fig. 2. "Conical refraction polarizer" of eight sectors applied in the sample beam of the interferometric setup. Green arrows indicate the orientation of the linear polarizer in each sector.

Two experiments analogous to the schemes presented in Figs. 1(a) and (b) are performed but now introducing the CRP in the sample beam, as expressed in the novel diagrams in Figs. 3(a) and (b). In both experiments the incident beam onto the entrance beam-splitter (non-polarizing) is RHC polarized light. In the first experiment, Fig. 3(a), no polarization element is inserted along the reference beam, whereas in the second experiment, Fig. 3(b), a linear polarizer with its transmission axis at $\beta_1 = 0°$ is introduced.

#237787 Received 9 Apr 2015; revised 10 Jun 2015; accepted 11 Jun 2015; published 2 Jul 2015

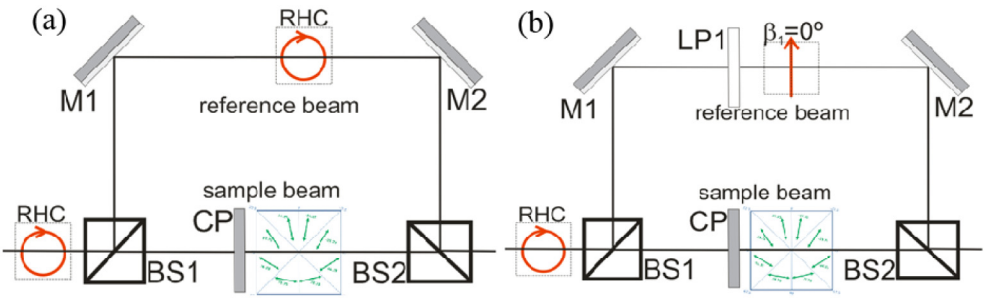

Fig. 3. Diagrams for the first (a) and second (b) experiment in the Mach-Zehnder setup, where the conical polarizer is indicated by the circle divided in eight sectors. The red arrows represent the Polarization state. The green arrows represent the transmission axis orientation of the conical polarizer.

In Fig. 4 we show the interferometric results for the experimental scheme in Fig. 3(a). Figure 4(a) corresponds to one of the four interferograms captured with the CCD camera, whereas in Fig. 4(b) we show the final processed pattern with the phase difference distribution map calculated across the aperture of the beam. Both in Figs. 4(a) and (b) we see very clearly the 4 lines (vertical, horizontal and diagonals) separating the eight sectors of the CRP. Note that the interference fringes show no discontinuities across the borders of the sectors, see Fig. 4(a). The processed phase map in Fig. 4(b) shows basically a constant gray level magnitude. The result in Eq. (7) indicated that no geometric phase arises from the interference between a RHC and a linearly polarized beam, thus a constant phase map is expected, thus agreeing with the results in Fig. 4.

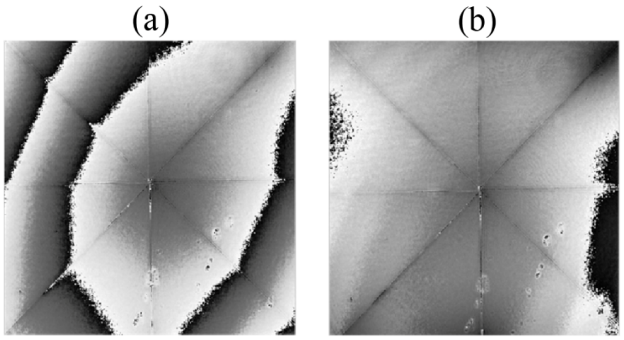

Fig. 4. Results for the experiment displayed in Fig. 3(a). (a) Sample interferogram. (b) Processed phase map pattern, where a constant phase-difference is obtained across the aperture.

In Fig. 5(a) we show one of the four interferograms captured in the second experiment, i.e. the one sketched in Fig. 3(b). In this case we see a discontinuity in the interference fringes across the bottom**:** two sectors where the minimum (maximum) in the interference fringes on one sector connects with the maximum (minimum) in the neighboring sector. This corresponds basically to the π radians phase jump calculated in Eq. (12). To ease the comparison we show the explicit diagram for the CRP in Fig. 5(b) and we note that the reference beam is linearly polarized along the vertical, i.e. $\beta_1 = 0°$. Then the two sectors at the bottom of the CRP produce linearly polarized light at angles $\beta_{2,\pm} = \pi/2 \pm \alpha$ for either sector, with $\alpha = 11.25°$. Once again, as in Fig. 4, the experimental results agree with the calculations in Section 2 and the phase difference across the aperture, and the phase jump, have purely a geometric phase origin.

#237787 Received 9 Apr 2015; revised 10 Jun 2015; accepted 11 Jun 2015; published 2 Jul 2015

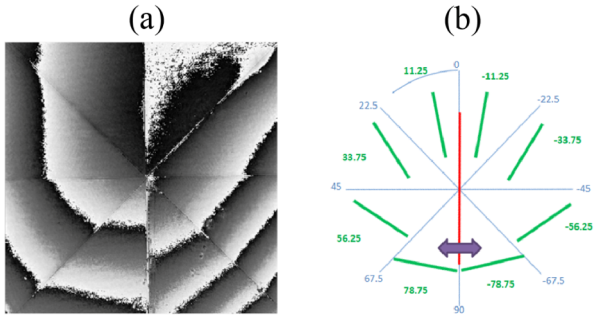

Fig. 5. Results for the experiment displayed in Fig. 3(b). (a) Sample interferogram where discontinuity in the fringes between the two bottom sectors is clearly visible. (b) CRP sector structure where the thick purple arrow indicates the two sectors at the bottom, whose transmission axis are almost orthogonal to the SOP in the reference beam, vertically polarized.

4. Experimental characterization of CR at the focal plane

Once the results obtained with the CRP for the two experiments (described in Fig. 3) have been evaluated we can proceed with the analogous experiments with the BC producing conical refraction in the sample beam. In Fig. 6 we show the scheme for the experimental setup, the Mach-Zehnder interferometer already described in Section 3 but with the adequate adaptations to incorporate the BC in the sample beam. Lens 1 (L1) is needed to produce a converging beam which passes along the optical axis of the BC, generating the conical refraction. Lens 2 (L2) is used to select and image with a certain magnification of the specific plane of interest onto the CCD camera. We are interested in the focal plane, which corresponds to the plane where the laser beam focuses and where the double ring structure described in the Introduction is produced. We see the detail of the mirrors (M1 and M2) along the reference beam, with the piezoelectric actuator (PZT) responsible for the phase-shift. The two beam-splitters (BS) used in the setup are non-polarizing.

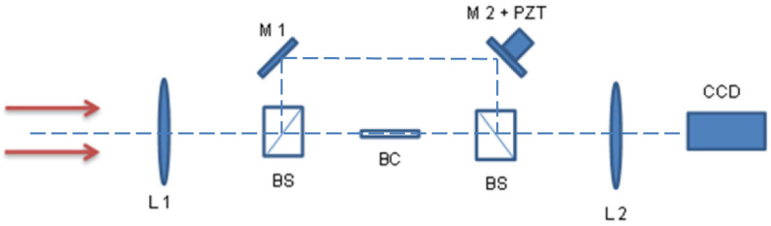

Fig. 6. Experimental setup for the Mach-Zehnder used to measure the phase distribution in the focal plane. An analogous setup is used for the CRP study. The CRP is illuminated with a collimated beam, and by means of lens L2 its image is formed at the CCD sensor plane.

The BC used in the setup was cut from a monoclinic centrosymmetric $KGd(WO_4)_2$ crystal [18]. Its polished entrances (cross section 6 mm × 4 mm) have parallelism with less than 10 arc sec, and they are perpendicular to one of the two optic crystal axes within a 1.5 mrad misalignment angle. Its length, l = 23.38 mm (measured with precision of less than 100 nm), and its conicity, α = 17 mrad, provide a CR ring of radius R_0 = 397 μm.

In Fig. 7 we show the continuously varying SOP distribution along the double ring structure exhibited in the focal plane. Images in Figs. 7(a) and (b) have been obtained using the setup sketched in Fig. 6 blocking the reference arm so that the CCD captures the intensity distribution in the focal plane. Before lens L1 a linear polarizer is located, thus the converging beam incident onto the BC has a uniform linearly polarized SOP. According to the CR phenomenon, each propagation direction of the electric field along the refraction cone is associated with a specific eigenpolarization [18]. Thus, if the incident SOP is orthogonally

#237787 Received 9 Apr 2015; revised 10 Jun 2015; accepted 11 Jun 2015; published 2 Jul 2015

polarized to the eigenpolarization in a specific propagation direction, then it is not transmitted in this direction. In Fig. 7(a) the incident electric field is linearly polarized along the vertical direction of the lab-reference system. We see that maximum brightness is observed in the bottom part of the ring, whereas no light appears at the top. In the case of Fig. 7(b) the incident SOP is linearly polarized at –45°: we see that no light is transmitted in the direction at + 45°. We observe the double ring structure in the focal plane with a null ring in the middle, the Poggendorf dark ring [18]. In the two bright rings, the eigenstates of polarization are the same. If we repeat this experiment for other linearly polarized states at the input we reconstruct the polarization eigenstates for the conical refraction along the azimuthal positions of the ring. These eigenpolarizations are shown in Fig. 7(c) and correspond to linearly polarized states, whose orientation evolves continuously from horizontally to vertically from the bottom to the top of the ring. This eigenpolarization distribution is equivalent to a spatially varying polarizer whose transmission axis coincides with the orientation of these eigenpolarizations. Thus, comparison between linear polarization orientation in Fig. 2, for the CRP, and in Fig. 7(c), for CR, shows that they are equivalent except for an azimuthal rotation of 180°. The other difference is that the CRP distribution is not continuous.

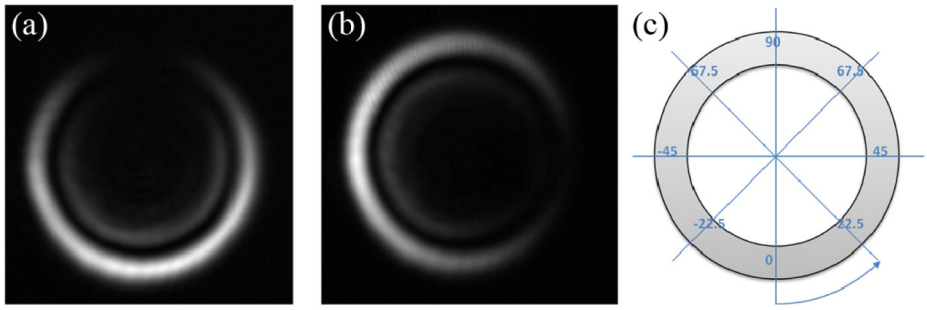

Fig. 7. Intensity distribution at the focal plane when a biaxial crystal is illuminated with linearly polarized light oriented (a) along the vertical, and (b) at –45°. In (c) we indicate the orientation of the linearly polarized eigenpolarizations along the azimuth of the ring.

Once the intensity profiles and the polarization structure exhibited by CR in the focal plane have been introduced, let us proceed with the interference experiments, sketched in Fig. 3. In Fig. 8 results from the scheme analogous to Fig. 3(a) are shown. Figure 8(a) corresponds to one of the four interferograms: a phase jump of π radians between the inner and outer bright rings is visible in the interference fringes. In Fig. 8(b) we provide the final phase map after processing the 4 interferograms with the phase-shifting algorithm: a clear contrast, corresponding to a phase difference of about π radians, is visible between the two rings. Additionally, along the azimuthal direction the gray level stays constant within each ring. According to the results obtained with the CRP in the equivalent experiment in Fig. 4, the geometric phase is invariant with the orientation of the linearly polarized state, which is then consistent with the constant azimuthal value both along the inner and along the outer rings. However, we have clearly shown the π radians phase jump between the two rings, at the null intensity ring, whose origin is not related with a geometric phase, but with a time delay, i.e. an optical path difference, generated by CR in the transmission along the BC. The corresponding numerical simulations obtained by means of the well-known Belsky-Khapalyuk-Berry [17,25] CR solution and the Jones vector formalism presented above are in good agreement with the experimental results, see Fig. 8(c). In Figs. 8(c) and 8(d) we present the numerically calculated instantaneous phase distribution and the transverse intensity pattern and polarization distribution (blue arrows) obtained when a circularly polarized Gaussian input beam is considered. Note that for a circularly polarized Gaussian input beam the theoretically calculated instantaneous intensity pattern presents a node along the rings, see Fig. 8(d).

#237787 Received 9 Apr 2015; revised 10 Jun 2015; accepted 11 Jun 2015; published 2 Jul 2015

However, the experimentally reported time averaged transverse intensity pattern results in a uniform intensity distribution along the rings due to the fact that this node rotates at the field frequency. As it can be observed, at the Poggendorff dark ring there is π radians phase jump in the electric field of the inner and outer CR rings, i.e. they have the same azimuth but opposite sense of the linear polarization.

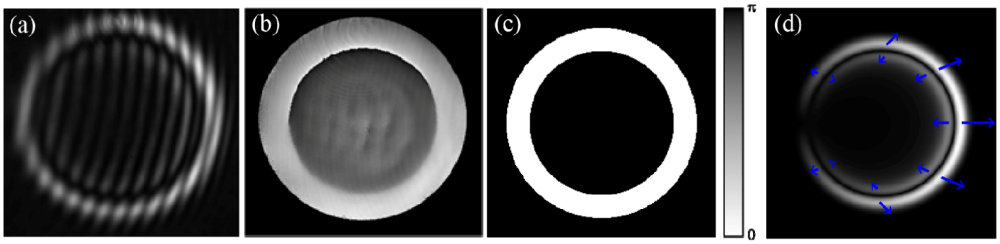

Fig. 8. Results at the focal plane for the experiment analogous to the one in Fig. 3(a). (a) Sample interferogram. (b) Experimentally processed and (c) numerically calculated phase map, where a constant phase-difference is obtained in the azimuthal direction, but a phase jump along the radial direction between the inner and outer rings is clearly visible. (d) Instantaneous transverse intensity and polarization distribution of the CR rings showing a change in the sense of the polarization between the inner and outer rings.

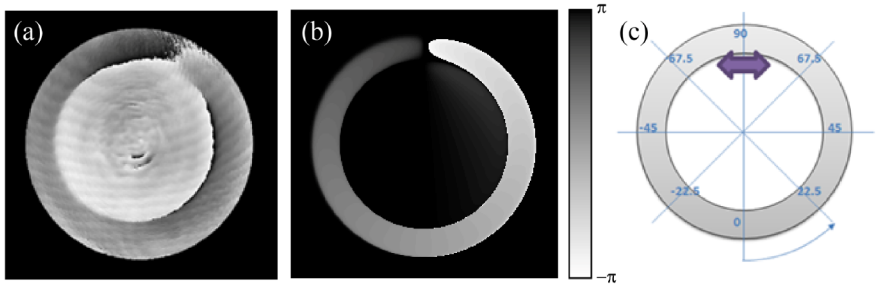

Fig. 9. Results at the focal plane for the experiments corresponding to the arrangement sketched in Fig. 3(b). (a) Experimentally processed and (b) numerically calculated phase map, where a discontinuity in the azimuthal direction near the top is visible. A second discontinuity, this one in the radial direction, is located in the null intensity ring between the inner and outer bright rings. (c) Orientation of the linearly polarized eigenpolarizations along the azimuth of the ring, where a thick purple arrow indicates where, approximately, the orientation is almost orthogonal to the SOP of the reference beam, horizontally polarized.

In Fig. 9 we show the results for the CR beam when applying the experimental scheme shown in Fig. 3(b). The processed phase map with the phase-shifting algorithm is shown in Fig. 9(a). As in Fig. 8(b) we see the gray level difference in the radial direction between the inner and outer rings, which corresponds to a π radians phase jump in the phase value. In the azimuthal direction we observe a phase jump near the top of the two rings (a few degrees clockwise with respect to the vertical). This is equivalent to the phase jump observed in Fig. 5 when using the CRP, which has a pure geometric origin. To ease the analysis, in Fig. 9(c) we show once again the diagram of Fig. 7(c) but now indicating explicitly with the thick purple arrow the approximate position where the eigenpolarizations are orthogonal to the orientation of the linearly polarized SOP from the reference beam, horizontally polarized. It is interesting to note that this geometric phase jump along the azimuthal direction is produced simultaneously both in the inner and outer rings, thus preserving the π radians phase difference along the radial direction between the inner and outer rings. Figure 9(b) shows the corresponding numerical simulations obtained by means of the well-known Belsky-Khapalyuk-Berry [17, 25] CR solution and the Jones vector formalism presented above. Both numerical simulations and experimental results are in excellent agreement. The main result

#237787 Received 9 Apr 2015; revised 10 Jun 2015; accepted 11 Jun 2015; published 2 Jul 2015

obtained is that both Figs. 8 and 9, corresponding to clearly different experiments with different geometric phase dependencies, show that there is a phase jump of π radians between the inner and outer bright rings, whose origin is not geometric but must be related to time delay.

4. Conclusions

The phase associated with the wavefront of a light beam is crucial when considering potential applications of structured beams. In this work, we have investigated in detail the phase structure of vector beams generated throughout the conical refraction (CR) phenomenon in biaxial crystals under the frequently used condition of well-developed rings with Poggendorff splitting. We have obtained that at the focal plane there is a phase jump of π radians between the inner and outer bright rings. By comparing this result with the one obtained with an azimuthally segmented linear polarizer that mimics the polarization structure of the CR rings, we have concluded that the origin of the π radians phase jump is not geometric but must be related to time delay, i.e. optical path difference in the transmission along the biaxial crystal. We have also obtained that along the azimuthal direction no phase evolution exists in the CR phenomenon apart from that of the geometric phase; i.e., at the focal plane the phase distribution obtained by CR is the same as that obtained with a sector polarizer.

Acknowledgments

We acknowledge financial support from the Spanish MINECO and Fondos FEDER (FIS2012-39158-C02-01, FIS2011-23719, BES-2010-031696, and AP2010-2310), and the Catalan Government (2014 SGR 1639). C. Iemmi appreciates the support from UBACyT 20020100100689, CONICET PIP 112-200801-03047, and ANPCYT PICT 2010-02179 (Argentina).

#237787 Received 9 Apr 2015; revised 10 Jun 2015; accepted 11 Jun 2015; published 2 Jul 2015